Label-Free DNA Detection Using a Charge Sensitive CMOS Microarray Sensor Chip

Javid Musayev, Yekbun Adlgüzel, Haluk Külah, Selim Eminoğlu, and Tayfun Akln

***Abstract*— This paper presents label-free DNA detection using a charge sensitive microarray sensor. The microarray sensor, fabricated with a standard CMOS process, contains 1024 detector elements integrated together with their readout circuit in a single chip. This microarray sensor chip is developed for biosensing applications involving label-free detection of charged particles and molecules with improved sensitivity. The proposed chip is used for the detection of DNA immobilization and hybridization by directly sensing the phosphate backbone charge of DNA molecules. The sensing part of the chip consists of an array of 7 μm × 7 μm capacitive metal electrodes arranged in 32 × 32 format with a pitch of 15 μm, which allows implementation of a portable and low-cost microarray sensor. The sensitivity of the microarray sensor is improved compared with other direct charge sensing CMOS biosensors, using low-noise detection and amplification circuits, and implementing correlated double sampling, which reduces the input referred rms noise level down to 6.8 electrons (e^-). Due to this low noise level, detection of DNA having 1 pM concentration is achieved, showing that the chip is much more sensitive than its counterparts, and even as sensitive as conventional fluorescence or gravimetric detection techniques. A dynamic range of 70 dB is achieved, along with the low noise level. The tests were performed with 10 base pairs DNA in 13-μM probe (5'-TCTCACCTTC-3') and 1-pM target (3'-AGAGTGGAAG-5') oligomer solutions. In both cases, charges of the DNA molecules interacting with the surface were successfully detected.**

***Index Terms*— Charge sensor, CMOS microarray, DNA, label-free detection.**

I. Introduction

IDENTIFICATION of human genome can prevent acquired genetic disorders like cancer, diabetes, cardiovascular diseases, and many others caused by DNA polymorphisms [1]. In this respect, genetic testing has become an important part of molecular biology in recent years, and a lot of effort has been spent to develop reliable, cost effective, and portable tools for DNA mutation analysis. Introduction of DNA microarrays since 1990s was the first step to genome wide screening. Various DNA detection methods are implemented in microarrays, which can be categorized in three main groups, as optical, gravimetric, and electrical. Optical detection methods are preferred for their high sensitivity. For example, fluorescence imaging is a conventional optical detection method in DNA microarrays [2]–[6], which has the sensitivity down to pM levels. However, fluorescence imaging requires bulky optical setup and fluorescent tagging. Another sensitive optical detection method is the surface plasmon resonance (SPR), which can achieve nM (even fM with enzymatic amplification) sensitivities. SPR does not normally require any kind of chemical tagging, but the need for an optical setup increases its cost [7]–[9]. The second detection method is gravimetric sensing realized with either quartz crystal microbalance devices (QCM) or mechanical resonators [10]–[12]. Detection relies on the change of natural frequency of the device due to the change in structural mass and/or damping factor upon DNA attachment, providing a high sensitivity (pM) without the need for any optics or chemical tagging. However, this method is not suitable for large format microarrays due to the size restrictions. Moreover, these sensors (especially QCM) require non-standard fabrication, resulting in decreased yield and increased cost. The third method is electrical detection, which can be implemented with CMOS chips offering high integration level required for microarray applications and low cost due to the well-developed integrated circuit fabrication techniques. Such electrical detection methods can be classified into two broad categories as impedance measurement and phosphate backbone charge sensing techniques. The former is to measure electrode-electrolyte interface impedance for sensing the changes on the electrode surface. The impedance change can be amplified with the use of red-ox enzymes [13]–[15], but usually this kind of chemical tagging is not required [16]–[23]. These methods offer sensitivities in the range of nM to sub–μM depending on the utilization of red-ox enzymes. A recent study [24] and [25] shows that sensitivity of this method can be significantly improved to fM levels; however, these kind of impedance measurement techniques have a problem of non-linearity. In addition, non-specific DNA targets in this study result in larger output variation than the specific ones due to the nature of the measurement technique. In the last few years, much more sensitive impedance based detection techniques have emerged due to the advancement in nanotechnology. In those techniques, ambient sensitive impedance of carbon nanotubes [26]–[30] or silicon nanowires [31]–[33]

Manuscript received July 5, 2013; revised September 14, 2013, December 17, 2013, and January 10, 2014; accepted January 11, 2014. Date of publication January 22, 2014; date of current version March 24, 2014. The associate editor coordinating the review of this paper and approving it for publication was Prof. Istvan Barsony.

J. Musayev was with the Middle East Technical University, Electrical and Electronics Engineering Department, Ankara 06800, Turkey. He is now with the Electrical and Computer Engineering Department, University of Toronto, Toronto, ON M5S 3J3, Canada (e-mail: cavid_f@yahoo.com).

Y. Adlgüzel is with the METU-MEMS Research and Application Center, Ankara 06532, Turkey (e-mail: yadiguzel@mems.metu.edu.tr).

H. Külah and T. Akın are with the Middle East Technical University, Electrical and Electronics Engineering Department, Ankara 06800, Turkey, and also with the METU-MEMS Research and Application Center, Ankara 06532, Turkey (e-mail: kulah@metu.edu.tr; tayfuna@metu.edu.tr).

S. Eminoğlu is with the Mikro-Tasarım Ltd., METU-Technopolis, Ankara 34306, Turkey (e-mail: eminoglu@metu.edu.tr)

Digital Object Identifier 10.1109/JSEN.2014.2301693

grown between two gold electrodes is measured, and DNA molecules immobilized on these nanostructures are detected due to the change in their impedance. Generally, sensitivity down to 10 fM target concentration is achieved, but in one particular example detection in 10^{-16} M was reported [34]. However, these sensors are limited by the ionic strength of the transport buffers and have low reproducibility [23]. Consequently, even though nanotubes and nanowires are promising, they are not yet available as a part of standard fabrication, hence their implementation is hard and production in high volumes is not very feasible due to the high device cost. The latter approach mentioned above is based on detection of the negative backbone charge of a DNA molecule. Such DNA detection can be realized by using ion sensitive field effect devices (ISFET technology) [35]–[38], offering μM level sensitivities in general. Although detection of a single nucleotide polymorphism in 100 pM was reported in one study [39], this study used an unconventional diamond gate ISFET, which is not feasible in standard CMOS processes, limiting its wide usage. As opposed to ISFET's, which measure the charge of DNA molecules indirectly, direct charge sensing, usually implemented by induction on capacitive electrodes, is used as well. Sensitivity levels as 2203 e^- [40], 100 pM [41] and 10^{-14} C (which is roughly 60000 e^-) [42] are reported with this technique.

This paper reports a novel CMOS sensor chip utilizing direct charge sensing technique [43] with improved sensitivity compared to its counterparts. Owing to a small detection capacitance and CDS, the CMOS microarray sensor achieves the rms noise level as low as 6.8 e^-. Considering that a single DNA bp possesses 1 or 2 e^- [44], theoretically one DNA molecule with 7 or 4 bp could be detected. The proposed sensor chip was tested, and hybridization process in 1 pM target concentration was successfully detected. The achieved 1 pM sensitivity is comparable with the sensitivity of the gravimetric or fluorescence imaging techniques, and such a sensitive detection of DNA has not yet been reported with any label free CMOS microarrays in literature, to the best of our knowledge. It should be noted that the 1 pM sensitivity is not a theoretical limit of the sensor, because the 6.8 e^- rms noise level can allow detection of a single DNA molecule, corresponding to 1.5×10^{-18} M in a 40 μL solution. However, currently the measured sensitivity is limited by chemical and biological factors like surface modification, immobilization/hybridization efficiencies, and applied protocol. Improving those can yield higher sensitivity levels.

The paper is organized as follows: Section II presents the structure of the detector element and explains the detection technique. Section III explains the readout mechanism and packaging of the fabricated sensor chip. Section IV describes test setup implemented to perform measurements. Section V reveals results of electronic performance measurements and DNA tests. Section VI provides a comprehensive discussion on the test results and Section VII concludes the paper.

II. Detector Element Structure and Operation

Fig. 1 shows the cross sectional structure of a detector element implemented in this study to realize DNA charge

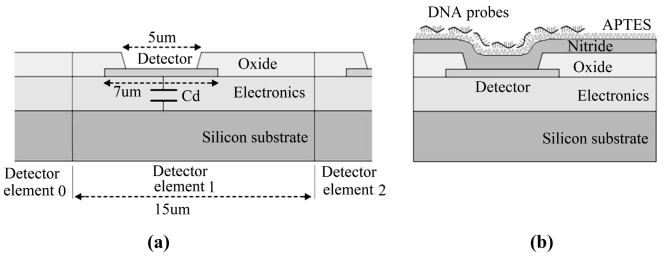

Fig. 1. The cross sectional structure of a detector element. (a) CMOS cross section and dimensions of a single detector element. (b) Post-CMOS surface modification. A 1 μm Si_3N_4 passivation layer is deposited and APTES polymer is incubated on the surface to enable DNA immobilization. DNA probes horizontally adsorbed to the surface of the detector element.

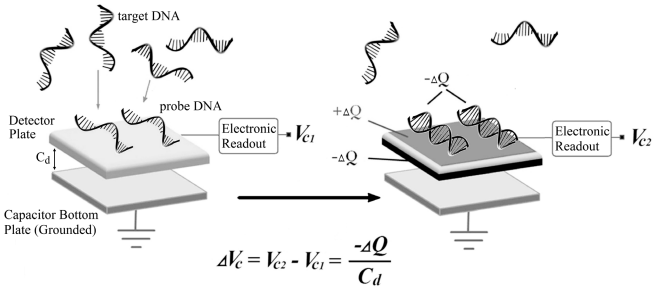

Fig. 2. Operation principle of a capacitive detector element. Hybridized target molecules induce a charge difference on the detector, which results in a voltage difference that is read out using on-chip and low-noise circuitry.

detection. The single element consists of a 7 μm $\times$ 7 μm capacitive detector implemented with the top metal of the CMOS process and the integrated circuitry required for the signal readout. 1024 of such detector elements are placed with 15 μm pitch in a 32 $\times$ 32 array format. 5 μm $\times$ 5 μm openings are formed on the oxide passivation over the capacitive detector. This is done to easily adjust the detector surface for different biological applications, e.g. gold coating for immobilizing samples with thiol (SH) group. However, in this study, electrical isolation of the detector from the sample solution is required to prevent electronic crosstalk between detector elements. Isolation is provided with a 1 μm nitride (Si_3N_4) passivation layer. The nitride layer is not suitable for DNA immobilization, therefore 3 Amino-Propyl-Triethoxy-Silane (APTES) polymer is deposited on the surface by overnight incubation in a 5 % silane solution in a nitrogen chamber (Terra Universal with Nitro Watch System and Dual Purge System). Then, the chip surface is washed with excess ethanol and dried over the heater plate for 1 hour, at 110 °C.

Fig. 2 illustrates the detection technique which relies on a direct charge sensing by reading the voltage of the capacitive detector on which the probes are immobilized. This voltage changes linearly with the amount of target molecules hybridized to the probes, because the negative charge of target molecules is induced on the detector, provided that the distance between the charge and the capacitor surface is much smaller than the width of the detector. This distance is determined by the thickness of nitride passivation layer and APTES, which are about 1 μm and 20 nm [45], [46] respectively.

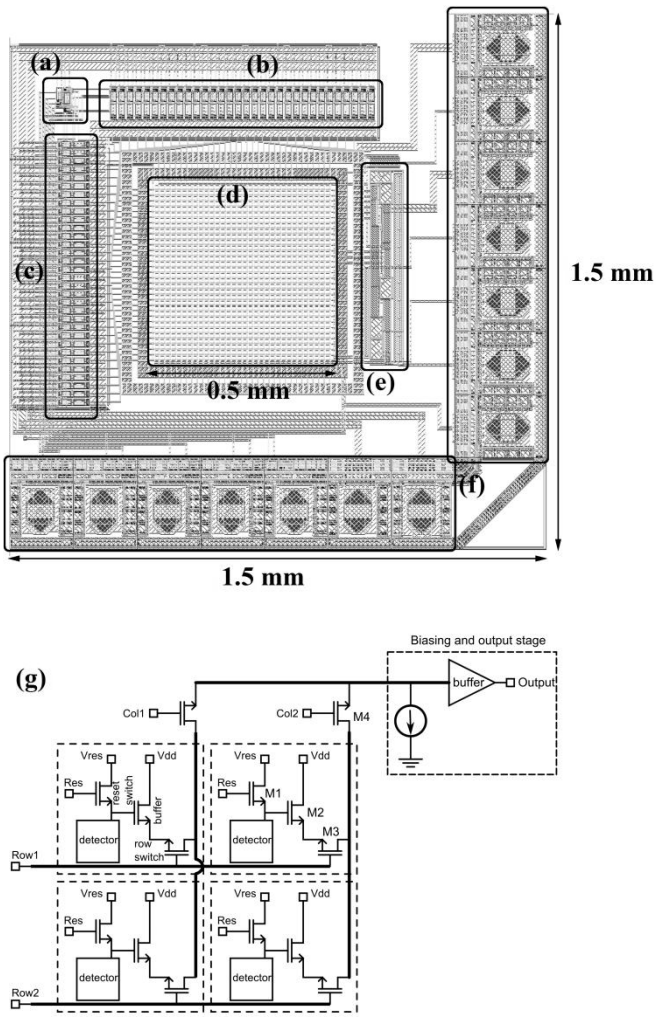

Fig. 3. Layout of the sensor chip and the circuitry of a detector element. (a) Control unit. (b) Horizontal scanner. (c) Vertical scanner. (d) 32 × 32 detector array. (e) Bias circuitry. (f) Bonding pads. (g) A 2 × 2 detector array showing the circuitry of a single detector element together with the bias circuitry.

The overall charge Q induced on the surface by a charge q can be calculated as in (1), for given detector width ($w = 7\ \mu$m) and separation distance ($d = 1\ \mu$m) [40].

$$Q = \frac{2q}{\pi}\arctan\left(\frac{w}{2\sqrt{3d}}\right) = 0.7 \tag{1}$$

Consequently, 70% of the charge attached to the surface is induced on detector.

Detector is a floating metal, so the induced charge results in a charge separation and changes the voltage of the capacitor C_d. The capacitor voltage is read out with the chip electronics to measure the amount of the induced charge. A charge difference of $-\Delta Q$ generates a voltage difference equal to $\Delta V_c = -\Delta Q/C_d$. Therefore, reducing the value of C_d results in a larger conversion gain, which is defined as the amount of voltage difference induced by a single electron, and improves the signal-to-noise ratio (SNR). The overall simulated capacitance of C_d is around 6 fF, corresponding to a 26 μV/e$^-$ conversion gain. In this respect, the CMOS technology is a good candidate for a sensitive and label free DNA microarray application, since an array of detector elements with very small capacitance and therefore very high conversion gain can be implemented and integrated with the required low–noise readout electronics.

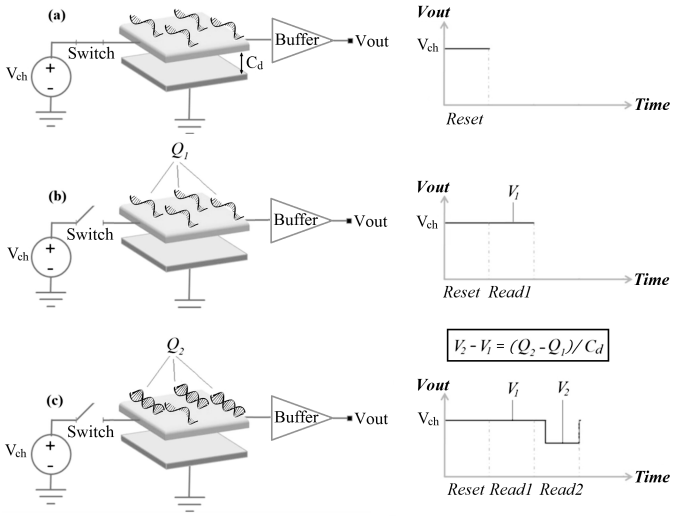

Fig. 4. The simplified schematic and readout mechanism of the detector element: (a) The switch is turned on and detector is reset to V_{ch} potential. (b) The switch is turned off and the first reading is done to record the reset value of the detector element (V_1). (c) Integrated DNA discharge the detector capacitor and the second reading is done to define the new voltage value (V_2). The voltage difference between the two readings (V_2-V_1) is proportional to the amount of charge (Q_2-Q_1) integrated on the detector surface with the coefficient of Cd.

III. Sensor Chip

A. Circuitry and Readout

The sensor chip is fabricated with a standard 0.35 μm CMOS process. Fig. 3 shows basic blocks of the chip on its layout and transistor level circuitry of a single detector element illustrated in a 2 × 2 representative detector array. The chip measures 1.5 mm × 1.5 mm including bonding pads, where the 32 × 32 array of detector elements occupies a 0.5 mm × 0.5 mm area. Array scanning is performed by digital blocks which are horizontal and vertical scanners, and the control unit. Analog bias circuitry located outside of the detector array realizes low noise biasing of the detector circuitry. I/O bonding pads provide interconnection with the external electronics.

Fig. 4 illustrates a simplified schematic and readout operation of a single detector element. Reset is applied periodically to restore the voltage of the detector to a V_{ch} value, because it drops while DNA hybridizes and its negative charge integrates on the detector. The buffer amplifier isolates detector capacitance from the capacitive loading of the rest of the readout circuits. During readout, the sensor capacitance is initially reset to V_{ch} potential [Fig. 4(a)]. Then the switch is turned off, and the reset value V_1 is recorded [Fig. 4(b)]. This is done to measure the precise value of the detector voltage before integration, as it would deviate from V_{ch} value after opening the switch due to charge injection, clock feed through, and the reset noise. Finally, the switch is kept off for charge

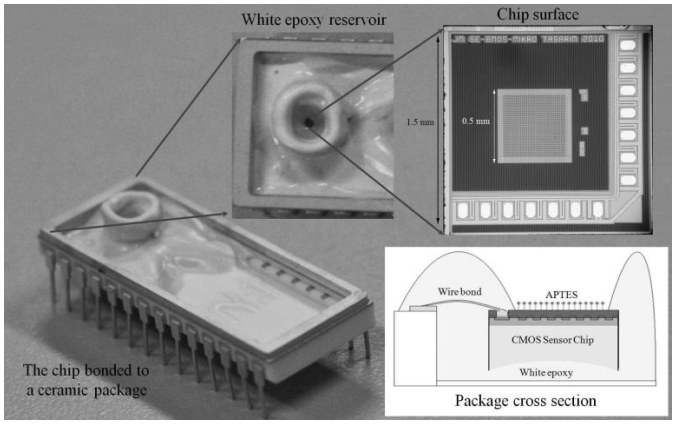

Fig. 5. Packaging of the sensor chip. The CMOS chip, which measures 1.5 mm × 1.5 mm is coated with a nitride layer. It is bonded to a ceramic package, and white epoxy is used to isolate the wire bonds and to form a reservoir for DNA solutions. The chip surface is modified with APTES polymer.

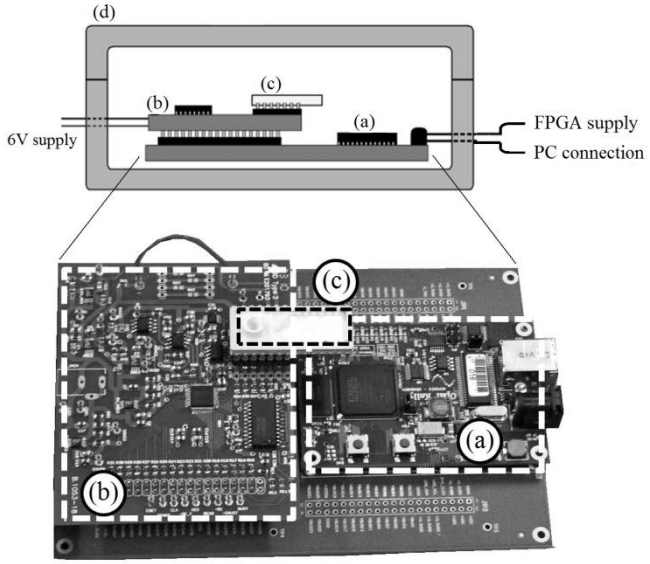

Fig. 6. The test setup. (a) Xilinx XM3010 FPGA board. (b) Custom made ADC board. (c) Sensor chip package. (d) Metal enclosure box-Faraday cage.

integration and the voltage of the detector reduces to V_2 due to the hybridized charges [Fig. 4(c)]. The difference of the two correlated readings (V_1 and V_2) is calculated with the external software and divided by the value of detection capacitor to identify the amount of immobilized charge. Such CDS significantly reduces the noise by eliminating the aforementioned electronic phenomena.

Addressing is realized with row switches implemented per each detector element and column switches implemented per each column. These switches are controlled by the row and column registers implemented on chip. The sensor chip also contains a control unit maintaining the synchronization and control of the system, an analog circuitry for biasing buffers, and input/output pads. The output of each detector element is sequentially transferred to the analog output pad and is processed by the external electronics.

B. Packaging

Fig. 5 shows the packaging of the sensor chip. The chip is wire bonded to a ceramic package by etching the nitride passivation over the bonding pads with laser (New Wave Research, LCSII 1064), and white epoxy (Loctite, Epoxy Patch, Henkel Corp., USA) is used to isolate the wire bonds and to build a reservoir on the chip surface for DNA solutions. The volume of the reservoir is sufficient to contain around 40 μL of sample solution on the sensor surface. The surface of the reservoir is covered with a stretch film during tests to prevent evaporation. Close-up view of the chip and the illustration of the package cross section are given for convenience. The package is suitable for being tested with a custom test electronics board.

IV. Test Setup

A. Electronics

Fig. 6 illustrates the test setup. Test electronics consists of an analog to digital converter (ADC) board, a field programmable gate array (FPGA-OPAL Kelly XM3010), a DC power source (HP Agilent E3631A) and a PC. The sensor chip package is plugged to the ADC board and its analog output corresponding to the sequentially ordered voltages of the 1024 detector elements is converted to an 18-bit digital data. The custom made ADC board is plugged to the FPGA board (Opal Kelly BRK3010 board). The FPGA provides synchronization and control of the digital signals required for proper operation of the chip and the ADC, stores the converted output data to its RAM, and transfers it to PC through a USB interface. The digital data is stored to PC and is easily processed. All electronic setup except for the power supply and PC is contained in a Faraday cage (a metal box) to prevent electromagnetic interference.

B. DNA Samples

The oligomers utilized throughout our tests were synthesized (Alpha DNA, Montreal, Quebec, Canada) as probes with 5'–TCTCACCTTC-3' sequence and fully complementary targets with 3'–AGAGTGGAAG–5' sequence. The probe oligomers comprised 5' thiol modification to be able to use the same oligomers in the tests of the prospective gold-coated chips as well. DNA samples were diluted in de-ionized (DI) water, separated into aliquots and kept in -20 °C for short term use.

V. Test Results

A. Electronic Performance

The electronic performance of the sensor chip is verified before performing DNA tests. The most critical performance parameters i.e. the noise, output voltage swing, and leakage of the chip are measured. Table I gives the summary of these measurements averaged for 1024 detector elements. The values of the measured parameters are given in volts, in electrons assuming a 26 μV/e$^-$ conversion gain, and in DNA assuming that a 10 bp DNA carries 20 electrons. All noise measurements

TABLE I
MEASURED ELECTRONIC PERFORMANCE PARAMETERS

Parameters	Volts ($\times 10^{-6}$)	Electrons	10 bp DNA
External electronics rms noise	**24**	0.9	0.05
Total rms noise without CDS	**1.02×10^{3}**	39.0	1.95
Total rms noise with CDS	**177**	6.8	0.34
Output voltage swing	**650×10^{3}**	25,000.0	1,250.00
Electronic leakage	**821**	32.0	1.60

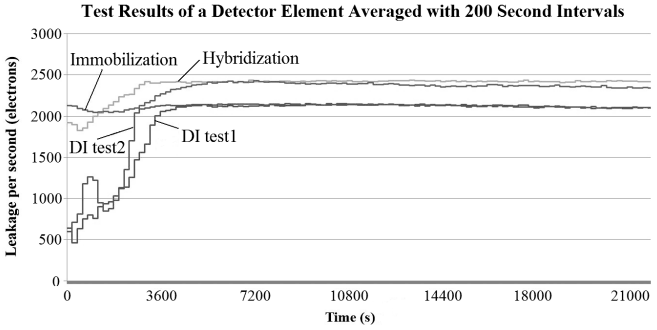

Fig. 7. Leakage levels of a representative detector element for all 4 tests, averaged with 200 second intervals. The leakage level during Immobilization and Hybridization exceeds the leakage level of DI tests, which indicates detection of DNA molecules.

are performed by finding the variance of ADC data collected for 5 minutes with the sampling rate of 100k SPS. The rms noise of the overall system is measured to be less than 7 e^-, in 1.5 MHz bandwidth defined by the output pole of the sensor. The rms noise of the external electronics was measured by disconnecting the chip output and giving a regulated DC voltage to the ADC input. This noise is measured to be only 0.92 e, verifying that external electronics do not dominate the overall noise. The rms noise level without CDS is 39 e, meaning that the CDS has a significant effect on noise reduction as expected. This result is reasonable as the theoretical reset noise for a 6 fF capacitor is 31 e^-_{rms}. The output voltage swing is measured to be 25000 e, corresponding to 70 dB dynamic range, which is sufficient noting that this value is updated in every two frames, i.e. 20 ms. The average electronic leakage is measured to be 32 e^-/frame at the frame period of 10 ms, by calculating the difference between the two output samples measured at two consecutive frames in case of zero DNA input. Since the leakage is much smaller than the voltage swing, it does not degrade the system performance.

According to the electronic performance measurements, the chip is suitable for DNA sensing applications requiring sensitivity down to 7 e. DNA tests were carried out after the verification of the chip performance.

B. Test With DI Water

Comparative tests were performed in dry environment and with DI water inside the reservoir to verify the isolation capability of the nitride passivation layer. Electrical isolation of detector elements is critical, because due to the 7 e sensitivity even the DI water acts as a conductive medium. Tests were performed for half an hour. The dry test was performed before, and the DI test after modifying the surface with APTES. The relative leakage performance of the detector elements was similar within each test, but the leakage values in DI test were about 30 % lower than in dry test. This is a result of increased capacitance due to existence of DI water layer, as the leakage current would result in smaller voltage change for higher capacitance. The difference in leakage values between detector elements can exist, which is a result of electronic leakage, gain, and capacitance variations due to process mismatches. However, this difference does not affect the measurements, because the amount of adsorbed charge is defined according to the variation of leakage value of any detector element during tests. Consequently, the initial value of the leakage is not important, and the system is suitable for performing the DNA tests.

C. Test With DNA Samples

Immobilization and hybridization tests were performed with intermediate washing steps and DI tests. Each test was done for about 8 hours to get comparative results. Overnight immobilization was done in a 40 μL, 13 μM probe DNA solution. Then the chip was rinsed with DI water and 8 hours DI test was performed. Hybridization test with a 40 μL, 1 pM target DNA was done afterwards. Then, another washing step and the DI test were performed.

Fig. 7 shows test results of an arbitrary detector element, fairly representing the system performance. The leakage/second values of all tests averaged with 200 second intervals are shown for initial 6 hours. Leakage values settle within 1.5 hours, which is probably related with the thermal, photonic, and mechanic disturbances introduced to the dynamics of the solution, as the cover of the Faraday cage was removed and a sample was added. To avoid the transient behavior, a better test setup can be designed to allow injection of a solution without disturbing the ambient parameters of the system (temperature, electromagnetic interference, etc.). The steady state data can still be analyzed to compare the leakage values in each case. It is clear that the leakage increased in case of immobilization and hybridization, and decreased during DI tests performed after washing.

Fig. 8 shows the leakage level of detector elements in electrons/second for each test. The leakage values were averaged for the test period excluding initial settling time of 1.5 hours. In Fig. 8(a), leakages of 10 different detector elements are shown. Although, there is a variation in the output levels of detector elements (due to process, post process, and electronic mismatches) the relative leakage variation between the tests is very similar for all detector elements. In Fig. 8(b), the average leakage of all 1024 detector elements is shown, to represent the overall performance. Error bars of $\pm1\sigma$ for the average leakage levels are shown in Fig. 8(c), where the leakage levels

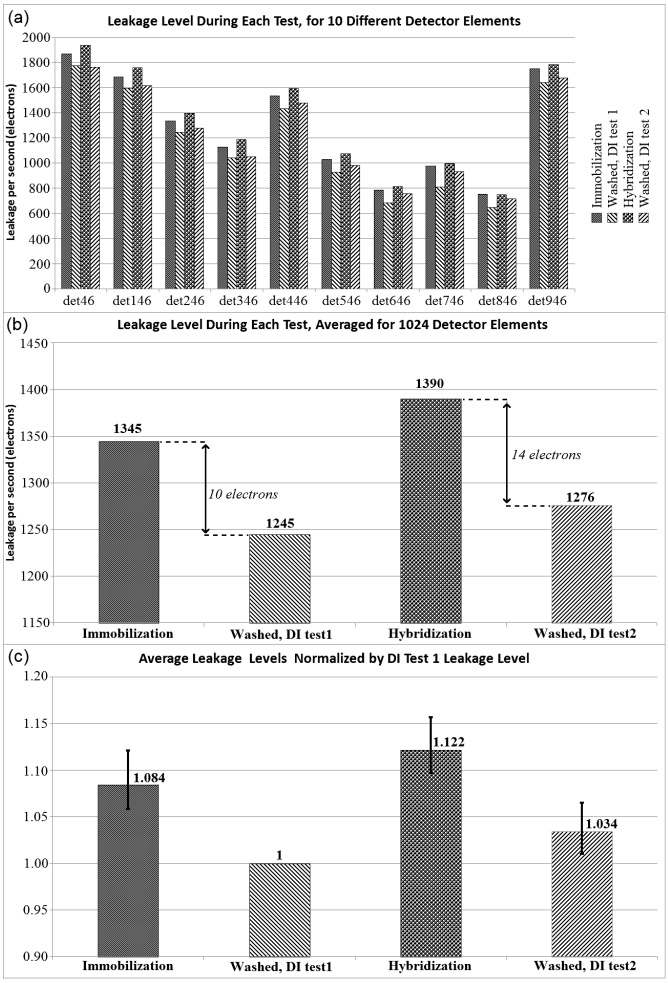

Fig. 8. Leakage levels (electrons per second) during each test: (a) for 10 randomly selected detector elements, (b) averaged for 1024 detector elements, and (c) normalized by the "DI Test 1" for each detector and then averaged. $\pm 1\sigma$ deviation is shown with the error bars. The difference between "Immobilization" and "DI Test 1" represents the average number of electrons induced on a detector element each second during the "Immobilization" test. Similarly, the difference between "Hybridization" and "DI Test 2" represents the number of electrons induced on a detector element each second during "Hybridization" test.

TABLE II
DNA TESTS- MEASURED AND ESTIMATED PARAMETERS

Parameters	Immobilization ($\times 10^6$ DNA)	Hybridization ($\times 10^6$ DNA)
Available locations on the sensor surface (estimated)	~2.0×10^3	~2.0×10^3
DNA molecules inside the solution (estimated)	312.0×10^6	24.0
DNA molecules interacted with the surface (measured)	**147.5**	**168.1**

are normalized by the DI Test 1 for each detector, thereby cancelling the variation illustrated in Fig. 8(a). Leakage levels of immobilization and hybridization tests were higher than the leakage levels of DI tests performed after washing the excess DNA. The difference between the DNA tests and DI tests

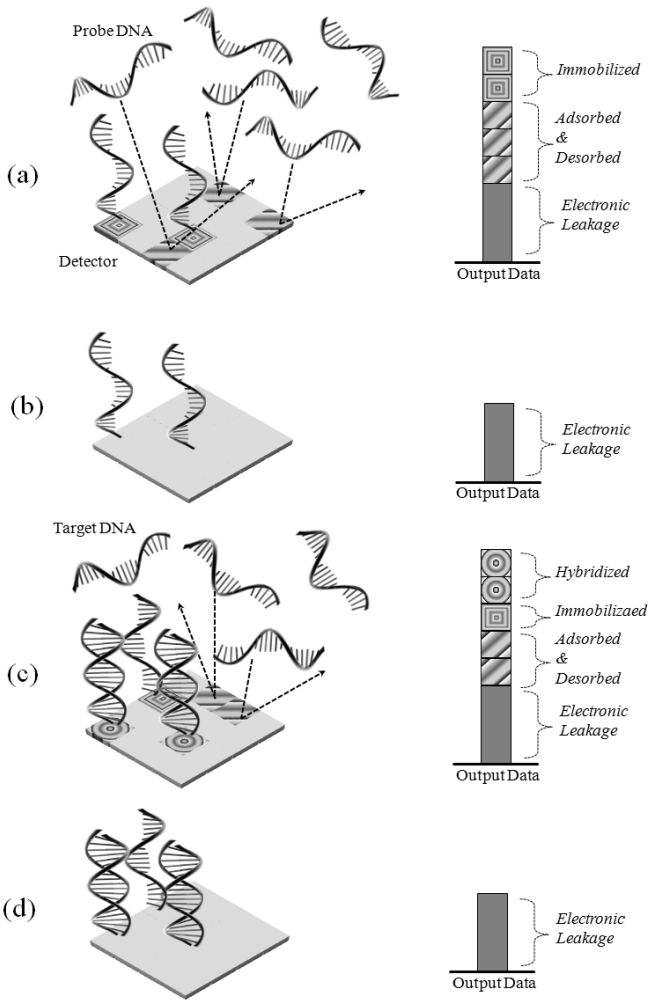

Fig. 9. Illustration of the expected surface processes and the resultant output data for each test. Gray pattern on the surface of the detector represents different events and the gray pattern of the output data is shown accordingly. The DNA adsorbs to APTES horizontally but vertical attachment is shown for better illustration. (a) Immobilization test. (b) The first DI test. (c) Hybridization test. (d) The second DI test.

are the effect of washing, which leads to the removal of free DNA molecules that can interact with or bind to the surface. Therefore, this difference represents the rate of induction of DNA electrons on a detector element in electrons/second. The difference for the immobilization test was slightly smaller than for the hybridization test, indicating that this rate was higher during hybridization.

Qualitative and quantitative discussion on these test results are provided in the next section. Observed behavior is meaningful considering the nature of immobilization-hybridization processes. Despite the complex nature of electrochemical interactions at the surface, an attempt is made to develop a theoretical model to estimate the number of hybridized DNA molecules according to the measurement results.

VI. DISCUSSION

Different processes that would occur during tests can change the surface charge density of detectors leading to the change of the output data. Fig. 9 represents expected processes and

the resultant output data for each test. For example, in the case of immobilization test [Fig. 9(a)] the output is the sum of electronic leakage, *immobilized*[1] DNA, and the molecules that are *adsorbed* to the surface and *desorbed* later due to the weak binding. Therefore, one molecule could be detected several times until it is firmly bonded. Similarly, in the case of hybridization test [Fig. 9(c)] the output results from target to probe *hybridization*,[2] target *immobilization* to free locations, and *adsorption & desorption* processes. Finally, the output in DI tests performed after washing the excess DNA [Fig. 9(b) and (d)], is the effect of electronic leakage only. When washing does not remove *immobilized* or *hybridized* molecules, these molecules do not result in any output data, since they exist on the surface from the beginning of the test and do not result in any change in the surface charge. Then, if the electronic leakage value calculated in the DI test is subtracted from the leakage value of the DNA test performed before, the number of DNA molecules which have interacted with the surface can be found. These interactions include *immobilization* + *adsorption & desorption* for the immobilization test, and *hybridization* + *immobilization* + *adsorption & desorption* for the hybridization test. The average rate of these interactions for each detector element can be extracted from Fig. 8 as *5 oligomer/s* and *5.7 oligomer/s* for immobilization and hybridization, respectively; assuming that each DNA oligomer has a charge of 20 e^-. This measurement proves that the DNA concentration of the solution does not affect the measurement, and the output is defined purely by the surface interactions, since the measured rate of surface interactions are close (*5 oligomer/s* and *5.7 oligomer/s*) in both cases, despite much higher concentration in case of immobilization (13 μM vs. 1 pM).

Table II gives the summary of calculations required for further analysis. Roughly 2 billion DNA molecules can be located on the surface of 1024 detectors measuring 7 um $\times$ 7 um, assuming a surface coverage density of 1 DNA per 5 nm $\times$ 5 nm area. The number of available DNA molecules in the 40 μL solution is 312×10^{12} DNA for 13 μM concentrated immobilization solution and 24×10^6 DNA for 1 pM concentrated hybridization solution. Finally, from the measured rate of surface interactions, the total number of DNA molecules interacted with the surface during 8 hours can be calculated as 147.5 million for the immobilization (*immobilized* + *adsorbed & desorbed*) and 168.1 million for the hybridization test (*immobilized* + *adsorbed & desorbed* + *hybridized*). Even assuming that all of the surface interacting molecules are the *immobilized* ones, less than 7.5 % of the available surface would be occupied by the end of the immobilization test. The reason for such small surface coverage despite excess DNA concentration maybe the slow dynamics of the *immobilization* in DI water as opposed to buffer solutions. Consequently, almost the same surface as in immobilization test is available for the DNA interactions during the hybridization test. Therefore, the rate of nonspecific interactions of the hybridization test can be assumed to be equal to the rate of overall surface interactions of the immobilization test. On the other hand, the number of DNA molecules interacting with the surface is about 7 times larger than the number of available molecules inside the solution in case of the hybridization test. This means that a single molecule is counted several times, in other words *adsorption & desorption* process dominates. The dominancy claims that the surface occupation was even smaller than 7.5 % during the immobilization test. Therefore, the DNA free locations are almost equal for both hybridization and immobilization tests, indicating that the initial assumption is reliable. As a result, the number of *hybridized* DNA molecules can be calculated as 20.6 million by taking the difference of surface interactions of the hybridization and immobilization tests. As expected, this value does not exceed the total number of available target DNA molecules in the solution which is 24 million.

The same DNA sequence was immobilized on the whole array in this study for testing purposes. However, various printing (spotting) techniques outlined in [47] exist for immobilizing unique oligonucleotides on different spots in the same array.

Gold coating of the detectors is aimed for the future work. Only probe molecules will be modified with the thiol group, which has affinity to gold stronger than that of DNA to APTES. Moreover, thiol modified molecules would immobilize vertically on the surface and thereby form a self assembled monolayer. These would significantly improve the immobilization efficiency and reduce the non-specific effects that complicate interpretation of the output data, since only probe molecules would be able to immobilize on the surface. These test results show that the proposed CMOS sensor array can be used for applications requiring low cost and sensitive DNA detection.

VII. Conclusion

This paper reports the design, fabrication, and testing of a 32 $\times$ 32 CMOS sensor array for a sensitive DNA immobilization and hybridization detection. A 6.8 e^-_{rms} noise level and 25000 e^- output swing were measured at 10 ms frame rate. A simple mask free post CMOS processing was required to perform the DNA detection tests, which was the deposition of a nitride layer for the isolation purpose and incubation of an APTES polymer on the sensor surface for DNA immobilization. This kind of surface modification is good for the proof of concept, but is not the best choice in terms of reducing non-specific binding. Implementation of gold coated detectors that are suitable for thiol modified DNA probe immobilization is aimed for the future work to improve the immobilization efficiency and reduce the non-specific effects. DNA immobilization and hybridization tests were performed, and their results were interpreted by developing a theoretical model for DNA-surface interaction processes. Although these electrochemical processes are quite complex and it is hard to extract hybridized molecule quantity from simple immobilization-washing-hybridization-washing steps with

[1]italic "*immobilization*" is not to be confused with the name of the immobilization test, as it indicates the process by which the DNA molecules are strongly adsorbed to the surface and not desorbed after washing.

[2]italic "*hybridization*" represents target DNA to probe DNA binding and is not to be confused with the name of the hybridization test.

a single DNA sequence, the low noise level of the sensors allows detection of the total amount of surface interacting charges with very high precision. Therefore, detection of the hybridized DNA molecules was possible even in 1 pM target DNA solution containing 10 bp oligomers. Perhaps, quantification can also be validated in the future, relying on the sensitivity, if a test procedure eliminating non–specific bindings and other surface effects is developed. This sensitivity is close to the detection level of optic and gravimetric detection methods and had not been achieved with any label free standard CMOS sensors before. Although detection was done in 1 pM solution, this is not a sensitivity limit of chip electronics. The measured noise level is sufficient to detect the charge of a single DNA molecule with 7 bp, i.e. the detection efficiency, which depends on the binding probability, is dominated by the surface treatment and applied protocol rather than the chip noise level. Relying on the promising performance of the chip, sub–pM sensitivity and SNP detection are aimed for the future work.

ACKNOWLEDGMENT

We thank O. Akar for the dicing and nitride coating of the microarray sensor chips.

REFERENCES

[1] K. M. Sweet and R. C. Michaelis, *The Busy Physician's Guide to Genetics, Genomics and Personalized Medicine*. New York, NY, USA: Springer-Verlag, 2011.

[2] T. C. Aitman, "DNA microarrays in medical practice," *Brit. Med. J.*, vol. 323, no. 7313, pp. 611–615, Sep. 2001.

[3] L. Cremonesi, M. Ferrari, P. Giordano, C. L. Harteveld, M. Kleanthous, T. Papassava, *et al.*, "An overview of current microarray-based human globin gene mutation detection methods," *Hemoglobin*, vol. 31, no. 3, pp. 289–311, 2007.

[4] F. Erdogan, R. Kirchner, W. Mann, H. H. Ropers, and U. A. Nuber, "Detection of mitochondrial single nucleotide polymorphisms using a primer elongation reaction on oligonucleotide microarrays," *Nucl. Acid Res.*, vol. 29, no. 7, p. 36, Apr. 2001.

[5] F. Gemignani, C. Perra, S. Landi, F. Canzian, A. Kurg, N. Tonisson, *et al.*, "Reliable detection of beta-talassemia and G6PD mutations by DNA microarray," *Clin. Chem.*, vol. 48, no. 11, pp. 2051–2054, Nov. 2002.

[6] M. J. Kozal, N. Shah, N. Shen, R. Yang, R. Fucini, T. C. Merigan, *et al.*, "Extensive polymorphisms observed in HIV-1 clade B protease gene using high density oligonucleotide arrays," *Nature Med.*, vol. 2, no. 7, pp. 753–759, Jul. 1996.

[7] T. T. Goodrich, H. J. Lee, and R. M. Corn, "Direct detection of genomic DNA by enzymatically amplified SPR imaging measurements of RNA microarrays," *J. Amer. Chem. Soc.*, vol. 126, no. 13, pp. 4086–4087, Mar. 2004.

[8] R. J. Heaton, A. W. Peterson, and R. M. Georgiadis, "The effect of surface probe density on DNA hybridization," *Nucl. Acids Res.*, vol. 29, no. 24, pp. 5163–5168, 2001.

[9] K. A. Peterlinz, G. M. Rosina, H. M. Tonya, and M. J. Tarlov, "Observation of hybridization and dehybridization of thiol tethered using two-color surface plasmon resonance spectroscopy," *J. Amer. Chem. Soc.*, vol. 119, no. 14, pp. 3401–3402, Apr. 1997.

[10] F. Caruso, E. Rodda, and D. N. Furlog, "Quartz microbalance study of DNA immobilization and hybridization for nucleic acid sensor development," *Anal. Chem.*, vol. 69, no. 11, pp. 2043–2049, Jun. 1997.

[11] L. J. Donald, D. J. Hosfield, S. L. Cuvelier, W. Ens, K. G. Standing, and H. W. Duckworth, "Mass spectrometric study of the *Escherichia Coli* repressor proteins, IcIR and GcIR, and their complexes with DNA," *Protein Sci.*, vol. 10, no. 7, pp. 1370–1380, Jul. 2001.

[12] Y. Okahata, Y. Matsunobi, K. Ijiro, M. Mukae, A. Murakami, and K. Makino, "Hyubridization of nucleic acids immobilizaed on quartz crystal microbalance," *J. Amer. Chem. Soc.*, vol. 114, no. 21, pp. 8299–8300, Oct. 1992.

[13] V. Dharuman, E. Nebling, T. Grunwald, J. Albers, L. Blohm, B. Elsholz, *et al.*, "DNA hybridization detection on electrical microarrays using coulostatic pulse technique," *Biosensors Bioelectron.*, vol. 22, no. 5, pp. 744–751, Dec. 2006.

[14] R. Thewes, F. Hofmann, A. Frey, B. Holzapfl, M. Schienle, C. Paulus, *et al.*, "Sensor arrays for fully electronic DNA detection on CMOS," in *Proc. ISSCC*, vol. 1. Feb. 2002, pp. 350–473.

[15] P. M. Levine, P. Gong, R. Levicky, and K. L. Shepard, "Real-time, multiplexed electrochemical dna detection using an active complementary metal-oxide-semiconductor biosensor array with integrated sensor electronics," *Biosensors Bioelectron.*, vol. 24, no. 7, pp. 1995–2007, Mar. 2009.

[16] S. Carrara, A. Cavallini, Y. Leblebici, G. De Micheli, V. Bhalla, F. Valle, *et al.*, "New probe immobilizations by Lipoate-Diethalonamines or ethylene-glycol molecules for capacitance DNA chip," in *Proc. 3rd IWASI*, vol. 3. Jun. 2009, pp. 9–14.

[17] C. Guiducci, C. Stagni, G. Zuccheri, A. Bogliolo, L. Benini, B. Samory, *et al.*, "DNA detection by integrable electronics," *Biosensors Bioelectron.*, vol. 19, no. 8, pp. 781–787, Mar. 2003.

[18] E. Ghafar-Zadeh, M. Sawan, and D. Therriault, "CMOS based capacitive sensor laboratory-on-chip: A multi disciplinary approach," *Analog Integr. Circuit Process.*, vol. 59, no. 1, pp. 1–12, Apr. 2009.

[19] C. Stagni, D. Esposti, C. Guiducci, C. Paulus, M. Schienle, M. Augustyniak, *et al.*, "Fully electronic CMOS DNA detection array based on capacitance measurement with on-chip analog-to-digital conversion," in *Proc. IEEE ISSCC*, Feb. 2006, pp. 69–78.

[20] C. Stagni, C. Guiducci, L. Benini, B. Riccò, S. Carrara, B. Samori, *et al.*, "CMOS DNA sensor array with integrated A/D conversion based on label-free capacitance measurement," *IEEE J. Solid-State Circuits*, vol. 41, no. 12, pp. 2956–2964, Dec. 2006.

[21] C. Stagni, C. Guiducci, L. Benini, B. Riccò, S. Carrara, B. Samori, *et al.*, "A fully electronic label free DNA sensor chip," *IEEE Sensors J.*, vol. 7, no. 4, pp. 577–585, Apr. 2007.

[22] S. B. Prakash and P. Abshire, "On-chip capacitance sensing for cell monitoring applications," *IEEE Sensors J.*, vol. 7, nos. 3–4, pp. 440–447, Mar. 2007.

[23] K.-H. Lee, S.-H. Choi, J.-O. Lee, M.-J. Sohn, J.-B. Yoon, and G.-H. Cho, "An autonomous CMOS hysteric sensor for the detection of desorption-free DNA hybridisation," *Biosensors Bioelectron.*, vol. 26, no. 11, pp. 4591–4595, Jul. 2011.

[24] W.-A. Lai, C.-H. Lin, Y.-S. Yang, and M. S.-C. Lu, "Ultrasensitive detection of avian influenza virus by using CMOS impedimetric sensor arrays," in *Proc. IEEE 25th Int. Conf. MEMS*, Feb. 2012, pp. 894–897.

[25] M. S.-C. Lu, Y.-C. Chen, and P.-C. Huang, "5 × 5 CMOS capacitive sensor array for detection of the neurotransmitter dopamine," *Biosensors Bioelectron.*, vol. 26, no. 3, pp. 1093–1097, Nov. 2010.

[26] A. Bonanni and M. del Valle, "Use of nanomaterials for impedimetric DNA sensors: A review," *Anal. Chem. Acta*, vol. 678, no. 1, pp. 7–17, Sep. 2010.

[27] A. R. Gao, N. Lu, X. L. Gao, P. F. Dai, T. Li, Y. B. Gong, *et al.*, "Label free DNA detection based on silicon nanowires," in *Proc. 16th Int. Conf. Solid-State Sensors, Actuat. Microsyst.*, Jun. 2011, pp. 2271–2274.

[28] S. Sorgenfrei, C. Y. Chiu, C. Nuckolls, and K. Shepard, "Ultra-sensitive carbon nanotubes for single-molecule detection of DNA hybridization kinetics using conductance-based correlation spectroscopy," in *Proc. 16th Int. Conf. Solid-State Sensors, Actuat. Microsyst.*, Jun. 2011, pp. 882–885.

[29] M. T. Martinez, Y.-C. Tseng, N. Ormategui, I. Loinaz, R. Eritja, and J. Bokor, "Label-free DNA biosensors based on functionalized carbon nanotube field effect transistors," *Nano Lett.*, vol. 9, no. 2, pp. 530–536, Jan. 2009.

[30] Y. Weizmann, D. M. Chenoweth, and T. M. Swager, "DNA-CNT networks for DNA detection," *J. Amer. Chem. Soc.*, vol. 133, no. 10, pp. 3238–3241, Feb. 2011.

[31] G. Zheng, F. Patolsky, Y. Cui, W. U. Wang, and C. M. Lieber, "Multiplexed electrical detection of cancer markers with nanowire sensor arrays," *Nature Biotechnol.*, vol. 23, pp. 1294–1301, Sep. 2005.

[32] G.-J. Zhang, J. H. Chua, R.-E. Chee, A. Agarwal, S. M. Wong, K. D. Buddharaju, *et al.*, "Highly sensitive measurements of PNA-DNA hybridization using silicon nanowire biosensors," *Biosensors Bioelectron.*, vol. 23, no. 11, pp. 1701–1707, Jun. 2008.

[33] C.-H. Lin, C.-H. Hung, C.-Y. Hsiao, H.-C. Lin, F.-H. Ko, and Y.-S. Yang, "Poly-silicon nanowire field-effect transistor for ultrasensitive and label-free detection of pathogenic avian influenza DNA," *Biosensors Bioelectron.*, vol. 24, no. 10, pp. 3019–3024, Jun. 2009.

[34] M. A. Bangar, D. Shirale, H. J. Purohit, W. Chen, N. V. Myung, and A. Mulchandani, "Single conducting polymer nanowire based sequence-specific, base-pair-length dependant label-free DNA sensor," *Electroanalysis*, vol. 23, no. 2, pp. 371–379, Feb. 2011.
[35] M. Barbaro, A. Bonfiglio, and L. Raffo, "A charge-modulated FET for detection of biomolecular processes: Conception, modeling, and simulation," *IEEE Trans. Electron Devices*, vol. 53, no. 1, pp. 158–166, Jan. 2006.
[36] S. Ingebrandt and A. Offenhausser, "Label-free detection of DNA using field-effect transistors," *Phys. Status Solidi A*, vol. 203, no. 14, pp. 3399–3411, Nov. 2006.
[37] D. S. Kim, Y. T. Jeong, H. J. Park, J. K. Shin, P. Choi, J. H. Lee, *et al.*, "An FET-type charge sensor for highly sensitive detection of DNA sequence," *Biosensors Bioelectron.*, vol. 20, no. 1, pp. 69–74, Jul. 2004.
[38] F. Uslu, S. Ingebrandt, D. Mayer, S. Bocker-Meffert, M. Odenthal, and A. Offenhausser, "Label free fully electronic nucleic acid detection system based on a field-effect transistor device," *Biosensors Bioelectron.*, vol. 19, no. 12, pp. 1723–1731, Jul. 2004.
[39] K.-S. Song, G.-J. Zhang, Y. Nakamura, K. Furukawa, T. Hiraki, J.-H. Yang, *et al.*, "Label-free DNA sensors using ultrasensitive diamond field-effect transistors in solution," *Phys. Rev. E*, vol. 74, no. 4, pp. 041919-1–041919-7, Oct. 2006.
[40] E. P. Anderson, "A CMOS label-free DNA microarray based on charge sensing," Ph.D. dissertation, Dept. Electr. Eng., Stanford Univ., Stanford, CA, USA, 2008.
[41] K.-H. Lee, J. O. Lee, S. Choi, J.-B. Yoon, and G.-H. Cho, "A CMOS label-free DNA sensor using electrostatic induction of molecular charges," *Biosensors Bioelectron.*, vol. 31, no. 1, pp. 343–348, Jan. 2012.
[42] S. Lai, A. Caboni, D. Loi, and M. Barbaro, "A CMOS biocompatible charge detector for biosensing applications," *IEEE Trans. Electron Devices*, vol. 59, no. 9, pp. 2512–2519, Sep. 2012.
[43] S. Eminoğlu and H. Külah, "Method and apparatus for biochemical sensor array with integrated charge based readout circuitry," U.S. Patent 850 551, Aug. 4, 2010.
[44] V. A. Bloomfield, D. M. Crothers, and I. Tinoco, *Nuclei Acids: Structure, Properties and Functions*. Sausalito, CA, USA: University Science, 1999.
[45] J. A. Howarter and J. P. Youngblood, "Optimization of silica silanization by 3-aminopropyltriethoxysilane," *Langmuir*, vol. 22, no. 26, pp. 11142–11147, Nov. 2006.
[46] E. T. Vanderberg, L. Bertilsson, B. Liedberg, K. Uvdal, R. Erlandsson, H. Elwing, *et al.*, "Structure od 3-aminopropyl triethoxy silane on silicon oxide," *J. Colloid Inter. Sci.*, vol. 147, no. 1, pp. 103–118, Nov. 1991.
[47] R. Don, *Microarray Biochip Technology*. Natick, MA, USA: Eaton Publishing, Apr. 2000, ch. 2, pp. 2–38.

Javid Musayev was born in Azerbaijan, in 1988. He received the B.Sc. and M.Sc. degrees in electrical and electronics engineering from Middle East Technical University in 2005 and 2009, respectively. From 2012 to 2013, he was an IC Design Engineer with MikroSens. Currently, he is pursuing the Ph.D. degree at the Department of Electrical and Computer Engineering, University of Toronto.

Yekbun Adlgüzel received the M.Sc. degree from the Pediatric Molecular Genetics Department, Ankara University Medical Faculty, Turkey, and the Undergraduate degree from the Molecular Biology and Genetics Department, Middle East Technical University (METU), Turkey. She received the Ph.D. degree from the Biophysics Department, Ruhr-University of Bochum, Germany, where he was involved in Postdoctoral studies in the Neurobiochemistry Department. She is currently a faculty member of the İstanbul Kemerburgaz University Medical Faculty, Turkey, and was a Postdoctoral Scientist with the BioMEMS Division, METU-MEMS Research and Application Center.

Haluk Külah received the B.Sc. and M.Sc. degrees in electrical engineering with high honors from Middle East Technical University (METU), Ankara, Turkey, in 1996 and 1998, respectively, and the Ph.D. degree in electrical engineering from the University of Michigan, Ann Arbor, in 2003. From 2003 to 2004, he was a Research Fellow with the Department of Electrical Engineering and Computer Science, University of Michigan. In 2004, he joined the Electrical and Electronics Engineering Department, METU, as a Faculty Member. His research interests include MEMS sensors, mixed-signal interface electronics design for MEMS sensors, bioMEMS, and MEMS-based energy scavenging. He is the Deputy Director of the METU-MEMS Center.

Selim Eminoğlu was born in Ankara, Turkey, in 1973. He received the B.Sc., M.Sc., and Ph.D. degrees in electrical engineering from Middle East Technical University (METU), Ankara, in 1996, 1998, and 2003, respectively. His Ph.D. thesis was focused on uncooled infrared focal plane arrays in standard CMOS technology. He received the METU Thesis of the Year Award in 2003, given by the Dr. M. N. Parlar Education and Research Foundation. From 1995 to 1998, he was a part-time Researcher with the VLSI Design Center, Information Technologies and Electronics Research Institute, Scientific and Technological Research Council of Turkey. From 1996 to 2003, he was a Teaching and Research Assistant with the Electrical and Electronics Engineering Department, METU. From 2003 to 2008, he was a Research Scientist with Teledyne Scientific and Imaging, LLC (formerly Rockwell Scientific), Thousand Oaks, CA, USA. From 2008 to 2011, he was an Assistant Professor with the Micro and Nanotechnology Department, Graduate School of Natural and Applied Sciences, METU, where he taught courses and co-supervised graduate studies in the area of imaging sensors and integrated circuits. He is the co-founder and CTO of Mikro-Tasarim Ltd., a fabless semiconductor company developing high performance imaging sensors for scientific and industrial applications. He has authored and co-authored over three journal papers, 12 conference papers, and holds three U.S. patents.

Tayfun Akln was born in Van, Turkey, in 1966. He received the B.Sc. degree in electrical engineering with high honors from Middle East Technical University, Ankara, Turkey, in 1987, and he moved for his graduate studies with a graduate fellowship provided by NATO Science Scholarship Program through the Scientific and Technical Research Council of Turkey in 1987. He received the M.Sc. and Ph.D. degrees in electrical engineering from the University of Michigan, Ann Arbor, in 1989 and 1994, respectively. Since 1995, 1998, and 2004, he has been an Assistant Professor, Associate Professor, and Professor with the Department of Electrical and Electronics Engineering, METU. He is the Director of the METU-Microelectromechanical Systems (MEMS) Center, which has a 1300 m^2 cleanroom area for $4''$, $6''$, and $8''$ MEMS process and testing. His research interests include MEMS, microsystems technologies, infrared detectors and readout circuits, silicon-based integrated sensors and transducers, and analog and digital integrated circuit design.

He has served in various MEMS, EUROSENSORS, and TRANSDUCERS conferences as a Technical Program Committee Member. He was the Co-Chair of the Nineteenth IEEE International Conference of MEMS in 2006, Istanbul, and he was the Co-Chair of the Steering Committee of the IEEE MEMS Conference in 2007. He is the winner of the First Prize in Experienced Analog/Digital Mixed-Signal Design Category at the 1994 Student VLSI Circuit Design Contest organized and sponsored by Mentor Graphics, Texas Instruments, Hewlett-Packard, Sun Microsystems, and Electronic Design Magazine. He is the co-author of the symmetric and decoupled gyroscope project, which won the first prize award in the operational designs category of the international design contest organized by DATE Conference and CMP in 2001. He is the co-author of the gyroscope project, which won the third prize award of 3-D MEMS Design Challenge organized by MEMGen Corporation (currently, Microfabrica).